

68. MINERAL ANALYSES FROM THE PERIDOTITE-GABBRO-BASALT COMPLEX AT SITE 334, DSDP LEG 37

D. B. Clarke, Department of Geology, Dalhousie University, Halifax, Nova Scotia, Canada

and

H. Loubat, Département des Sciences de la Terre, Université de Québec à Montréal, Montréal, P.Q.

ABSTRACT

Fifty-one analyses of silicates, oxides, and sulfides from a suite of ultrabasic and basic rocks at Site 334 are presented. The intrusive rocks show rhythmic, cryptic, and phase layering and are closely analogous to the Rhum-layered intrusion. The extrusive rocks are mineralogically similar to the intrusives, but are unlikely to be genetically related to them.

INTRODUCTION

Drilling at Site 334 penetrated ~50 meters of basalts which overlie at least 68 meters of gabbros and peridotites. The basalts are generally aphyric, or sparsely porphyritic containing phenocrysts of olivine, clinopyroxene, and plagioclase. The presence of very coarse grained rocks at shallow depth under the basalts is in itself surprising and significant. The peridotites show well-developed cumulus textures in which olivine and spinel are always cumulus phases, whereas two pyroxenes and plagioclase are cumulus phases only in the gabbros. The present mineral analyses were undertaken to determine if the gabbros and peridotites are the complements of the overlying basalts, i.e., if there is a genetic relationship between the intrusive rocks below and the extrusive rocks above.

All analyses were done by electron microprobe (Cambridge Microscan MK-5) using natural minerals as standards. The raw data were processed using the EMPADR VII correction procedure of Rucklidge and Gasparrini (1969).

MINERAL ANALYSES

Analyses of silicate minerals appear in Tables 1-3 and are graphically represented in Figure 1. In addition, Table 4 contains analyses of chrome spinels from the three peridotite specimens investigated. Also a qualitative petrographical investigation is summarized in Table 5. Finally, some of the rocks were briefly studied for their sulfide mineralogy and the following two analyses were made in gabbro 334-21-1, 47-49 cm:

	Pyrite	Chalcopyrite
Fe	47.83	30.63
Cu	-	34.54
Ni	0.07	0.03
S	53.27	34.26
	101.18	99.47

In other rocks, the following sulfides were identified but not quantitatively analyzed: 22-2, 61-63 cm;

pentlandite; 23-1, 127-129 cm; pyrrhotite; 24-3, 112-114 cm; chalcopyrite, pyrite, pentlandite. In many cases the sulfides appear to occur as disseminated blebs enclosed within the primary silicate minerals.

DISCUSSION

Within the limitations of the visual core descriptions (Aumento and Melson, 1974) and the low degree of core recovery, there appear to be at least nine cycles of peridotite-olivine gabbro-gabbro in the plutonic complex of Site 334. A cycle usually begins with peridotite, but in some cases the most basic member may be olivine gabbro. Also, a cycle usually ends with olivine-poor or olivine-free gabbro, but in some cases the cycle ends while the gabbro is still relatively olivine rich. This kind of rhythmic layering is found in several layered basic intrusions from the terrestrial environment (Wager and Brown, 1968). It remains to be seen what the nature of the cryptic layering is and which terrestrial model most closely applies to the submarine sequence.

In Table 6 the samples are arranged in stratigraphic order and the mineral chemistry is presented in summary form. Samples 22-2, 61-63 cm and 21-1, 47-49 cm are from the same rhythmic unit, and it is apparent that there is normal cryptic variation from the peridotite to the gabbro, i.e., increasing Fs molecule in the pyroxenes. There is also elimination of olivine, presumably through a reaction relationship with the liquid at the 1 atmosphere invariant point, $Ol^- + Opx^+ + Cpx^+ + Plag^+ + Liquid^-$. This reaction is strongly suggested by a careful petrographic examination: among the various episodes of crystallization, there is evidence of intensive replacement, suggested by frequent lobate contacts between olivine relics, pyroxenes, and plagioclase. It is also evident that whereas gabbro 21-1, 47-49 cm is the uppermost gabbro in the sequence, it is not the most differentiated. The most evolved gabbro in terms of its Fs content in the pyroxenes is 23-1, 127-129 cm. A more primitive gabbro, 24-3, 112-114 cm, is found deeper in the sequence.

The reversal in the Fs content of the pyroxenes (and An content of the plagioclase) hints that the nine

TABLE I
Microprobe Analyses of Olivines

	1	2	3	4	5	6	7	8
Fo	88.506	88.495	83.157	88.637	85.283	85.746	87.512	87.804
Fa	11.254	11.279	16.446	10.884	14.295	13.989	12.382	12.116
Larn	0.240	0.227	0.397	0.479	0.422	0.265	0.106	0.080
Fo	88.719	88.696	83.489	89.063	85.644	85.463	87.274	87.551
Fa	11.281	11.304	16.511	10.937	14.356	13.943	12.348	12.081
Niol	0.000	0.000	0.000	0.000	0.000	0.594	0.378	0.368
F/M	0.127	0.127	0.198	0.123	0.168	0.163	0.141	0.138
F/FM	0.113	0.113	0.165	0.109	0.144	0.140	0.124	0.121

Note: 1 = 26-1, 20-22 cm; olivine 5. 2 = 26-1, 20-22 cm; olivine 6. 3 = 15-2, 20 cm; olivine 1. 4 = 15-2, 20 cm; olivine 2. 5 = 20-2, 140-145 cm; olivine 1. 6 = 24-3, 112-114 cm; olivine 1. 7 = 22-2, 61-63 cm; olivine 1. 8 = 22-2, 61-63 cm; olivine 2.

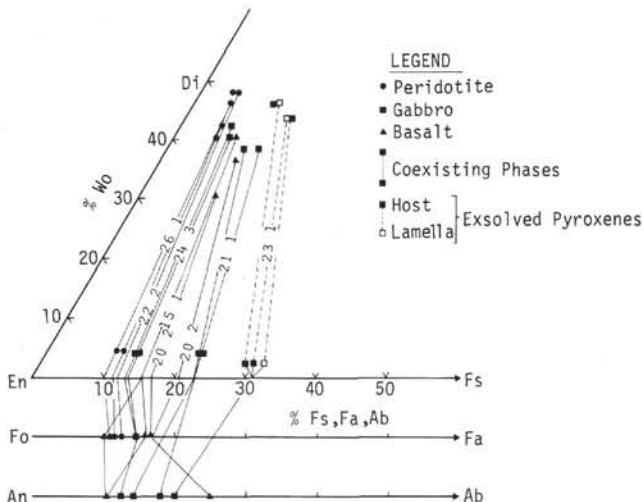


Figure 1. Mineral analyses for intrusive and extrusive rocks at Site 334.

rhythmic units are not the result of fractional crystallization of a single magma as is the case in the Skaergaard intrusion. Instead, the cyclical variation of rock types and mineral chemistry suggests that this complex has formed in a manner similar to that described for the Rhum-layered intrusion by Brown (1956). It is believed that these cumulates formed in a magma chamber that acted as a temporary reservoir for magmas en route to the surface. The longer the magma stayed in the reservoir, the more evolved would become both the cumulate pile and the erupted basalt.

There is no compelling mineralogical evidence to prove or disprove a genetic link between the basalts and the underlying intrusives. The basalts are more erratic in their mineral chemistry principally because most phenocrysts in the basalts suggest that, if there is a genetic link, these basalts were erupted from the magma chamber at a stage of evolution between gabbros of the types 24-3, 112-114 cm and 21-1, 47-49 cm. However, more convincing evidence exists against the idea that there is any genetic relationship between the intrusives and extrusives at Site 334. First, the close spatial relationship between the two groups makes unlikely the notion that the coarse-grained intrusives could be in situ cumulates from the same magmas that gave rise to the basalts. Secondly, the numerous breccia zones noted in the core logs, plus the cataclastic tex-

tures in the gabbros, suggest that these cumulates were tectonically emplaced. The greater the degree of displacement this type of deformation represents, the less likely it is that the intrusives and extrusives are genetically related. Among the breccias, the mysterious nannofossil chalk matrix could tentatively be explained by a process of "oblique diapirism" of ultramafic lenses being serpentized. The degree of serpentization of olivine is a direct function of the amount of olivine in these rocks (i.e., a dunitic layer is totally serpentized, and an olivine-poor gabbro has fresh olivine). If serpentization occurred with an increase of volume, it could result in a dislocation of the layered sequence, across an oblique serpentization front (Loubat, 1973). Lenses of brecciated serpentinites would eventually reach very superficial levels of the oceanic floor (Figure 2).

CONCLUSIONS

The conclusions listed below are tentative because of the gaps in the core record and because of the limited mineral data.

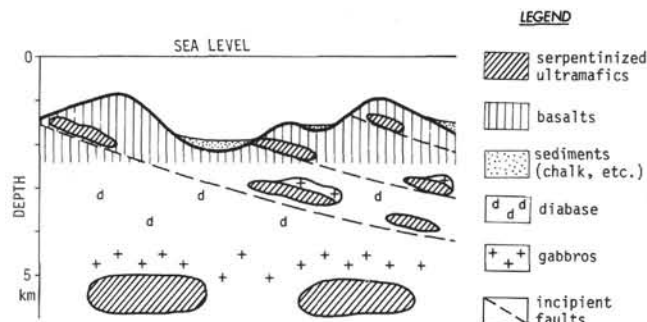


Figure 2. Proposed shallow cross-section of the oceanic floor at some distance away from the axis of a volcanic ridge. Due to steeply oblique isotherms and serpentinitization fronts, a lateral increase of volume and dislocation of ultramafic layers could occur. Some of these bodies in the process of serpentinitization will eventually be dragged in a phenomenon of "oblique diapirism," and they could reach levels of superficial basalts and sediments, in a process of incipient dislocation of the oceanic floor. This could account for the differential degree of serpentinitization of the layered body, the obvious increase of volume in the serpentinitization, and the breccias with chalky fossiliferous matrix.

TABLE 2
Microprobe Analyses of Pyroxenes

	1	2	3	4	5	6	7	8
SiO ₂	53.69	53.32	54.37	52.36	52.61	42.33	53.47	53.51
TiO ₂	0.20	0.32	0.20	0.40	0.30	0.41	0.21	0.37
Al ₂ O ₃	1.19	1.75	0.70	1.55	2.24	1.84	1.14	2.97
Cr ₂ O ₃	0.07	0.09	0.05	0.09	0.14	0.08	0.06	1.33
Fe ₂ O ₃	0.00	0.00	0.00	0.00	0.00	0.00	0.00	0.00
FeO	18.85	7.63	19.53	8.50	7.07	8.54	20.29	2.72
MnO	0.23	0.25	0.24	0.22	0.20	0.23	0.29	0.00
MgO	25.09	14.85	24.50	14.97	14.94	14.38	23.35	16.35
CaO	0.65	22.23	0.72	21.53	21.65	21.62	1.10	21.98
Na ₂ O	0.07	0.26	0.08	0.26	0.27	0.26	0.09	0.90
K ₂ O	0.02	0.04	0.03	0.05	0.05	0.06	0.03	0.03
Sum	99.98	100.74	100.42	99.93	99.46	99.75	100.03	100.16
Si	1.966	*	1.961	*	1.985	*	1.950	*
Al	0.034	2.000	0.039	2.000	0.014	2.000	0.050	2.000
Al	0.014	*	0.037	*	0.016	*	0.018	*
Ti	0.006	*	0.009	*	0.005	*	0.011	*
Cr	0.002	*	0.003	*	0.001	*	0.003	*
Fe ³⁺	0.000	*	0.000	*	0.000	*	0.000	*
Fe	0.578	*	0.235	*	0.597	*	0.265	*
Mn	0.007	*	0.008	*	0.007	*	0.007	*
Mg	1.369	1.975	0.814	1.105	1.334	1.961	0.831	1.134
Ca	0.026	*	0.876	*	0.028	*	0.859	*
Na	0.005	*	0.019	*	0.006	*	0.019	*
K	0.001	0.031	0.002	0.895	0.001	0.035	0.002	0.880
O	6.000	*	6.000	*	6.000	*	6.000	*
WO	1.293		45.512		1.439		43.947	
EN	69.426		42.295		68.102		42.510	
FS	29.281		12.193		30.459		13.543	
WO	1.285		44.898		1.429		43.377	
HYP	98.465		54.152		98.284		55.675	
JD	0.250		0.950		0.287		0.948	
F/M	0.427		0.298		0.453		0.327	
F/FM	0.299		0.229		0.312		0.246	
	9		10		11		12	
SiO ₂	55.73		55.92		50.55		51.20	
TiO ₂	0.11		0.11		0.22		0.24	
Al ₂ O ₃	2.14		2.16		3.69		3.17	
Cr ₂ O ₃	0.77		0.74		1.27		1.27	
Fe ₂ O ₃	0.00		0.00		0.00		0.00	
FeO	6.79		6.69		3.64		3.36	
MnO	0.00		0.00		0.11		0.10	
MgO	31.48		32.15		18.52		17.99	
CaO	2.53		2.19		19.56		20.75	
Na ₂ O	0.03		0.05		0.15		0.20	
K ₂ O	0.01		0.02		0.06		0.07	
Sum	99.59		100.03		97.77		98.35	
	14		15		16			
Si	1.948	*	1.944	*	1.880	*	1.896	*
Al	0.052	2.000	0.056	2.000	0.120	2.000	0.104	2.000
Al	0.036	*	0.032	*	0.042	*	0.034	*
Ti	0.003	*	0.003	*	0.006	*	0.007	*
Cr	0.021	*	0.020	*	0.037	*	0.037	*
Fe ³⁺	0.000	*	0.000	*	0.000	*	0.000	*
Fe	0.198	*	0.194	*	0.113	*	0.014	*
Mn	0.000	*	0.000	*	0.003	*	0.003	*
Mg	1.640	1.899	1.666	1.915	1.027	1.228	0.993	1.178
Ca	0.095	*	0.082	*	0.779	*	0.823	*
Na	0.002	*	0.003	*	0.011	*	0.014	*
K	0.000	0.097	0.001	0.086	0.003	0.793	0.003	0.841
O	6.000	*	6.000	*	6.000	*	6.000	*

1) The sequence of nine rhythmic units in the intrusive rocks at Site 334 appears to be the product of a Rhum, rather than a Skaergaard, type of fractional crystallization.

2) Cryptic variation is present in the uppermost intrusive unit, and it probably exists in each of the

rhythmic units. A detailed study of the phase chemistry of each rhythmic unit is suggested in order that the full record of evolution may be understood.

3) There is phase layering in many of the units; olivine and chrome spinel are frequently observed at the bottom, but not the top, of individual rhythmic

TABLE 2 - *Continued*

	9	10	11	12	13	14	15	16	
WO	4.901	4.200	40.510	42.872	38.293	37.979	4.023	3.911	
EN	84.833	85.784	53.491	51.709	50.738	49.105	74.105	74.255	
FS	10.266	10.016	5.899	5.419	10.969	12.916	21.872	21.834	
WO	4.896	4.193	40.310	42.485	37.991	37.657	4.015	3.903	
HYP	94.999	95.634	59.131	56.774	61.495	61.821	95.950	96.061	
JO	0.105	0.173	0.559	0.741	0.514	0.522	0.036	0.036	
F/M	0.121	0.117	0.114	0.108	0.222	0.270	0.297	0.295	
F/FM	0.108	0.105	0.102	0.097	0.181	0.212	0.229	0.229	
	17	18	19	20	21	22	23	24	25
SiO ₂	52.24	51.12	52.14	54.93	55.20	52.58	52.90	52.41	51.92
TiO ₂	0.43	0.00	0.00	0.34	0.33	0.40	0.41	0.29	0.33
Al ₂ O ₃	3.70	5.58	3.81	1.68	1.80	2.68	2.55	2.61	3.25
Cr ₂ O ₃	0.00	0.00	0.00	0.40	0.40	0.66	0.57	0.83	0.72
Fe ₂ O ₃	0.00	0.00	0.00	0.00	0.00	0.00	0.00	0.00	0.00
FeO	5.80	6.48	6.60	8.47	8.33	4.91	4.29	3.44	3.17
MnO	0.15	0.00	0.00	0.38	0.37	0.34	0.34	0.12	0.23
MgO	17.88	18.40	20.88	31.13	30.80	18.72	17.35	16.26	16.20
CaO	19.90	17.85	14.71	2.42	2.46	19.63	20.27	23.29	23.35
Na ₂ O	0.18	0.14	0.13	0.14	0.15	0.27	0.27	0.40	0.21
K ₂ O	0.06	0.00	0.00	0.08	0.08	0.09	0.09	0.06	0.06
Sum	100.34	99.57	98.27	99.97	99.92	100.28	99.04	99.50	99.44
Si	1.902	*	1.868	*	1.913	*	1.942	*	1.913
Al	0.098	2.000	0.132	2.000	0.087	2.000	0.066	2.000	0.058
AI	0.060	*	0.108	*	0.078	*	0.004	*	0.016
Ti	0.012	*	0.000	*	0.000	*	0.009	*	0.019
Cr	0.000	*	0.000	*	0.000	*	0.011	*	0.011
Fe ³⁺	0.000	*	0.000	*	0.000	*	0.000	*	0.019
Fe	0.177	*	0.198	*	0.202	*	0.249	*	0.245
Mn	0.005	*	0.000	*	0.000	*	0.011	*	0.011
Mg	0.970	1.223	1.002	1.308	1.142	1.422	1.634	1.919	1.615
Ca	0.776	*	0.699	*	0.578	*	0.091	*	0.093
Na	0.013	*	0.010	*	0.009	*	0.010	*	0.010
K	0.003	0.792	0.000	0.709	0.000	0.587	0.004	0.104	0.004
O	6.000	*	6.000	*	6.000	*	6.000	*	6.000
WO	40.364	36.800	30.076	4.624	4.748	39.653	42.446	47.926	48.283
EN	50.453	52.772	59.391	82.744	82.702	52.606	50.542	46.548	46.601
FS	9.183	10.428	10.533	12.632	12.558	7.742	7.012	5.525	5.116
WO	40.004	36.609	29.932	4.575	4.697	39.055	41.783	47.480	47.728
HYP	59.342	62.871	69.589	94.946	94.785	59.973	57.210	51.732	51.495
JD	0.655	0.520	0.479	0.479	0.518	0.972	1.007	0.733	0.777
F/M	0.187	0.198	0.177	0.160	0.159	0.157	0.150	0.123	0.118
F/FM	0.157	0.165	0.151	0.138	0.137	0.136	0.130	0.109	0.105

Note: 1 = 23-1, 127-129 cm; OPX host 1. 2 = 23-1, 127-129 cm; CPX lamella 1A. 3 = 23-1, 127-129 cm; OPX host 2. 4 = 23-1, 127-129 cm; CPX lamella 2A. 5 = 23-1, 127-129 cm; CPX host 3. 6 = 23-1, 127-129 cm; CPX host 4. 7 = 23-1, 127-129 cm; OPX lamella 4A. 8 = 26-1, 20-22 cm; OPX 3. 9 = 26-1, 20-22 cm; OPX 7.10 = 26-1, 20-22 cm; OPX 8. 11 = 26-1, 20-22 cm; CPX 9. 12 = 26-1, 20-22 cm; CPX 10. 13 = 21-1, 47-49 cm; CPX 1. 14 = 21-1, 47-49 cm; CPX 2. 15 = 21-1, 47-49 cm; OPX 3. 16 = 21-1, 47-49 cm; OPX 4. 17 = 15-2, 30 cm; CPX 1. 18 = 20-2, 140-145 cm; CPX 3. 19 = 20-2, 140-145 cm; CPX 4. 20 = 24-3, 112-144 cm; OPX 2. 21 = 24-3, 112-144 cm; OPX 3. 22 = 24-3, 112-114 cm; CPX 4. 23 = 24-3, 112-114 cm; CPX 5. 24 = 22-2, 61-63 cm; CPX 3. 25 = 22-2, 61-63 cm; CPX 4.

units. This phase layering is attributed to reaction relationships in a fractionating magma rather than settling of dense crystals in rhythmic units developed by "turbidity currents" in the magma chamber.

4) The mineral chemistry alone is not sufficient to establish or disprove a genetic link between the basalts and the underlying intrusives.

5) A genetic link between intrusives and extrusives is unlikely because of the close spatial association of the rocks and because of the deformation of the intrusives suggesting that they have been tectonically emplaced.

REFERENCES

Aumento, F. and Melson, W.G., 1974. DSDP Leg 37 visual core descriptions and sample distribution for igneous

cores, Holes 332A, 332B, 333A, 334, 335: DSDP Leg 37 Shipboard Report.

Brown, G.M., 1956. The layered ultrabasic rocks of Rhum, inner Hebrides: Phil. Trans. Roy. Soc. London, Series 240B, p. 1-53.

Loubat, H., 1973. Soubassement des dorsales volcaniques océaniques: Suisse Min. Pétrol. Bull., v. 53, p. 337-354.

Rucklidge, J. and Gasparrini, E.L., 1969. Electron microprobe analytical data reduction: Dept. of Geology, Institute of Toronto, Canada.

Wager, L.R. and Brown, G.M., 1968. Layered igneous rocks: Edinburgh (Oliver and Boyd).

TABLE 3
Microprobe Analyses of Feldspars

Note: 1 = 23-1, 127-129 cm; plagioclase 5. 2 = 23-1, 127-129 cm; plagioclase 6. 3 = 21-1, 47-49 cm; plagioclase 5. 4 = 21-1, 47-49 cm; plagioclase 6. 5 = 21-1, 47-49 cm; plagioclase 7. 6 = 21-1, 47-49 cm; plagioclase 8. 7 = 15-2, 20 cm; plagioclase 1. 8 = 20-2, 140-145 cm; plagioclase 1. 9 = 20-2, 140-145 cm; plagioclase 2. 10 = 24-3, 112-114 cm; plagioclase 6.

TABLE 4
Microprobe Analyses of Spinel

	1	2	3	4	5	6
SiO ₂	0.00	0.00	0.00	0.00	0.01	0.02
TiO ₂	0.37	0.40	0.66	0.70	0.63	0.52
Al ₂ O ₃	24.66	22.10	21.58	21.59	21.64	20.65
Fe ₂ O ₃	2.77	3.93	4.73	4.62	5.05	5.16
FeO	15.52	18.68	17.51	17.83	19.26	20.62
Cr ₂ O ₃	43.12	43.33	42.86	43.50	42.41	42.91
MnO	0.29	0.37	0.36	0.36	0.37	0.41
MgO	13.39	10.94	11.73	11.74	10.61	9.60
ZnO	0.00	0.00	0.00	0.00	0.00	0.00
CaO	0.02	0.02	0.02	0.02	0.01	0.02
Sum	100.14	99.77	99.45	100.36	99.89	99.91
Si	0.000	*	0.000	*	0.000	*
Ti	0.068	*	0.075	*	0.124	*
Al	7.064	*	6.522	*	6.369	*
Cr	8.288	*	8.580	*	8.486	*
Fe ³⁺	0.507	15.926	0.741	15.918	0.891	15.871
Fe	3.155	*	3.913	*	3.667	*
Mn	0.060	*	0.078	*	0.076	*
Mg	4.852	*	4.084	*	4.379	*
Zn	0.000	*	0.000	*	0.000	*
Ca	0.005	8.072	0.005	8.080	0.005	8.128
O	32.000	*	32.000	*	32.000	*
CHRO	52.260		54.156		53.895	
SPIN	44.545		41.169		40.444	
MAGN	3.195		4.675		5.661	
USP	0.886		1.027		1.683	
SPIN	92.481		88.880		86.245	
MAGN	6.634		10.903		12.072	
USP	0.763		0.082		1.308	
CHRO	93.519		91.315		89.311	
MAGN	5.718		7.883		9.381	
F/M	0.663		0.977		0.855	
F/FM	0.399		0.494		0.461	
					0.870	1.038
					0.465	0.509
						0.551

Note: 1 = 26-1, 20-22 cm; spinel 1. 2 = 26-1, 20-22 cm; spinel 2. 3 = 26-2, 5-10 cm; spinel 1. 4 = 26-2, 5-10 cm; spinel 2. 5 = 22-2, 61-63 cm; spinel 6. 6 = 22-2, 61 63 cm; spinel 7.

TABLE 5
Summary of Petrography

Sample (Interval in cm)	Rock Type	Modal Analysis	Grain Size (mm)	Texture	Alteration	
15-2, 20	Basalt	Plagioclase Clinopyroxene Olivine	50 45 5	Phenocrysts <3 Groundmass <1	Porphyritic (phenocrysts of Plag, Cpx, Oliv)	Minor chlorite in vesicles
20-2, 140-145	Basalt	Plagioclase Clinopyroxene Quench crystals Olivine	5 5 90 Tr	<1	Microporphyritic rock consisting mainly of quench crystals in vario- litic texture	Fresh
21-1, 47-49	Anorthositic gabbro	Plagioclase Clinopyroxene	60 40	1-6	Plagioclase-Cpx adcumulate; ex- solution in Cpx	Minor sericite
22-1, 17-23	Gabbro	Plagioclase Pyroxene	60 40	Phenocrysts <3	Cumulus plago- clase; intercumulus pyroxene	Partially amphi- bolitized
22-2, 61-63	Peridotite	Olivine Clinopyroxene Rodingite	70 15 15	Olivine 10-20 Cpx 1-4mm	Cumulus olivine; intercumulus Cpx with minor ex- solution	Olivine 95% serpentinized
22-2, 80-82	Peridotite	Olivine Clinopyroxene Orthopyroxene Chromite	60 18 22 Tr	Olivine 1-2 Cpx 8-15	Cpx exsolved; olivine cumulus pyroxenes inter- cumulus; mesh	Olivine and ortho- pyroxene partly serpentinized
23-1, 46-54	Peridotite	Olivine Iddingsite Opx Cpx Plag	60 40	Olivine 10-12	Olivines corroded; exsolution lamellae in fresh Cpx	Olivine totally serpentinized, Opx-Cpx-Plag serpentinized and rodingitized
23-1, 91-93	Gabbro	Plagioclase Clinopyroxene	50 50	<2	Ophitic; minor cataclasis; plagioclase cumu- lus; clinopyroxene intercumulus	Fresh
23-1, 127-129	Noritic gabbro	Plagioclase Pyroxenes	40 60	3-15	Adcumulate; augite and inverted pigeonite both with exsolution lamellae; cata- clastized	Fresh
23-2, 78-82	Peridotite	Olivine Orthopyroxene Plagioclase Chromite	70 15 15 Tr	<2	Trace of exso- lution in altered Opx	Olivine and ortho- pyroxene totally serpentinized; plagioclase rodingitized
24-2, 105-107	Olivine gabbro	Olivine Plagioclase Clinopyroxene	15 50 35	Generally <4	Plag poikilitic in Cpx	Olivine partly alter- ed to serpentine and iddingsite
24-3, 112-114	Olivine leucogabbro	Olivine Plagioclase Pyroxenes	5 55 40	1-6	Adcumulate	Olivine partly serpentinized
24-4, 100-106	Olivine gabbro	Olivine Plagioclase Pyroxenes	35 20 45	Olivine <10 Plag <2 Pyroxene 4	Opx and Cpx zoned, exsolved and with kink bands; olivine and plagioclase cumulus	Olivine partly serpentinized
26-1, 20-22	Peridotite	Olivine Pyroxenes Rodingite Spinels	60 30 5 5	3-10	Cumulus olivine and spinel; inter- cumulus plago- clase mesh; bastite; pyroxenes with exsolution	Olivine altered to serpentine

TABLE 5 - *Continued*

Sample (Interval in cm)	Rock Type	Modal Analysis		Grain Size (mm)		Texture	Alteration
26-1, 70-75	Peridotite	Olivine	65	Generally <10		Cpx with exsolution lamellae;	Olivine totally
		Clinopyroxene	22			Olivine cumulus;	serpentinized;
		Orthopyroxene	13			Cpx intercumulus	Opx partly
		Chromite	Tr				serpentinized
26-2, 5-10	Peridotite	Olivine	80	2-3		Cumulus olivine	Olivine totally
		Pyroxenes	15			and spinel;	serpentinized;
		Rodingite	5			intercumulus	Opx partly
		Spinel				pyroxenes and	serpentinized
						plagioclase; mesh;	
						bastite	
26-2, 56-71	Olivine gabbro	Olivine	20	<4		Exsolution lamellae	Olivine partly
		Plagioclase	40			in pyroxenes;	serpentinized
		Pyroxenes	40			cumulus plagioclase	
						(and olivine?)	
26-2, 59-64	Olivine gabbro (Pyroxenite)	Olivine	10	<3		Plagioclase cumulus;	Olivine
		Plagioclase	20			pyroxenes with	serpentinized
		Pyroxenes	70			exsolution	
						lamellae	

TABLE 6
Summary of Mineral Chemistry for Intrusive Rocks at Site 334

Depth (m)	Cycle	Rock Type	Sample (Interval in cm)	Phase Chemistry
310 -				
-				
-				
-		G		Olivine absent
315 -		G	21-1, 47-49	Wo ₃₈ En ₅₀ Fs ₁₂ Gabbro
-		G		Wo ₄ En ₇₄ Fs ₂₂
-		G		An ₈₀₋₈₅
-		G		
-		G		
320 -		G		
-		G		
-		G		
-*		G	22-1, 17-23	
-*		G		
325 -		P		Fo ₈₇
-		P	22-2, 61-63	Wo ₄₈ En ₄₇ Fs ₅ Peridotite
-*		P	22-2, 80-82	Cr ₅₄ Sp ₄₀ Mt ₆
-		G	23-1, 46-54	
-*		G	23-1, 91-93	
330 -		G	23-1, 127-129	Olivine absent
-		P		Wo ₄₄ En ₄₂ Fs ₁₄
-		G		Wo ₄₂ En ₆₇ Fs ₃₁ Gabbro
-		P		An ₈₀
-*		G		
-*		P		
335 -		G	23-2, 78-82	
-		P		
-		G		
-		G		
-*		G		
340 -*		G		
-*		OG	24-2, 105-107	Fo ₈₅
-*		OG		Wo ₁ En ₅₁ Fs ₈
-		OG	24-3, 112-114	Wo ₅ En ₈₃ Fs ₁₂ Gabbro
-*		OG		An ₈₈
345 -		OG		
-		OG		
-		OG		
-*		OG		
-		OG	24-4, 100-106	
350 -*		P		
-		P		
-		P		
-		P		
-		G		
335 -		G		
-		G		
-		G		
-		G		
-		G		
360 -		G		Fo ₈₈
-		G		Wo ₄₂ En ₅₃ Fs ₅ Peridotite
-*		P	26-1, 20-22	Wo ₄ En ₈₅ Fs ₁₁
-*		P		Cr ₅₄ Sp ₄₀ Mt ₅
-		P	26-1, 70-75	
365 -*		P	26-2, 5-10	Cr ₅₃ Sp ₄₃ Mt ₄ Peridotite
-		OG	26-2, 56-71	
-		OG	26-2, 59-64	
-		G		
-		G		
370 -		G		
		OG		

Note: P = Peridotite; OG = Olivine Gabbro; G = Gabbro; * = Breccia.